environments

Article

Superior Adsorption of Chlorinated VOC by Date Palm Seed Biochar: Two-Way ANOVA Comparative Analysis with Activated Carbon

Rania Remmani [1,2,*], Marco Petrangeli Papini [2], Neda Amanat [3] and Antonio Ruiz Canales [4]

[1] Sciences of the Matter Department, University of Biskra, Biskra 07000, Algeria
[2] Department of Chemistry, Sapienza University of Rome, 00185 Rome, Italy; marco.petrangelipapini@uniroma1.it
[3] Natural Resources Research Institute, University of Minnesota Duluth, Duluth, MN 55455, USA; amanat.n@gmail.com
[4] Engineering Department, Miguel Hernández University, 03202 Orihuela, Spain; aruizcanales@gmail.com
* Correspondence: rania.remmani@univ-biskra.dz

Abstract: This study explores biochar (BC) derived from date palm seeds as a high-performance adsorbent for the removal of trichloroethylene (TCE) and tetrachloroethylene (PCE) from aqueous solutions, with comparative analysis against commercial activated carbon (AC). The optimized BC, characterized by a high BET surface area of 654.79 m^2/g and unique nanotube morphology, demonstrated superior adsorption capacities of 86.68 mg/g for TCE and 85.97 mg/g for PCE, significantly surpassing the AC under identical conditions. Kinetic studies identified the pseudo-second-order model as the best fit, indicating chemisorption as the dominant mechanism. Isotherm modeling revealed a combination of multilayer and monolayer adsorption processes, underscoring the complexity of the BC's adsorption behavior. Statistical analysis via two-way ANOVA further validated the BC's significant superiority over the AC ($p < 0.0001$) for both contaminants. These results highlight the potential of date-palm-seed-derived biochar as a sustainable and cost-effective adsorbent for eco-friendly water treatment, emphasizing its role in reducing environmental impact and operational costs in real-world applications.

Keywords: biochar; chlorinated solvents; adsorption kinetics; isotherms; statistical analysis; nanotube morphology

check for updates

Citation: Remmani, R.; Papini, M.P.; Amanat, N.; Canales, A.R. Superior Adsorption of Chlorinated VOC by Date Palm Seed Biochar: Two-Way ANOVA Comparative Analysis with Activated Carbon. *Environments* **2024**, *11*, 288. https://doi.org/10.3390/environments11120288

Academic Editor: Janusz Kozinski

Received: 29 October 2024
Revised: 8 December 2024
Accepted: 13 December 2024
Published: 14 December 2024

Copyright: © 2024 by the authors. Licensee MDPI, Basel, Switzerland. This article is an open access article distributed under the terms and conditions of the Creative Commons Attribution (CC BY) license (https://creativecommons.org/licenses/by/4.0/).

1. Introduction

CVOCs, including TCE and PCE, are notorious environmental pollutants commonly utilized in industrial activities such as dry cleaning, degreasing, and chemical manufacturing. These compounds are hazardous due to their toxicity, carcinogenic properties, and resistance to biodegradation in both aqueous and soil environments [1]. Their persistence, particularly in groundwater systems, poses significant challenges as they can migrate over large distances, creating long-term contamination risks for ecosystems and human health [2,3]. As a result, finding effective and sustainable remediation strategies for CVOCs is critical for safeguarding water quality and public health [4].

Among the various methods available for removing CVOCs from water, adsorption has garnered widespread attention due to its simplicity, efficiency, and cost-effectiveness [5,6]. AC is widely recognized for its high adsorption capacity, attributed to its large surface area and porosity [7]. However, the reliance on non-renewable resources and energy-intensive processes in the production of AC raises environmental concerns [8,9]. This has prompted growing interest in bio-based adsorbents, particularly BC, which is derived from renewable agricultural waste and offers a more sustainable alternative [10].

BC is produced via the pyrolysis of biomass under limited oxygen conditions, yielding a carbon-rich material with a tunable surface structure and chemical composition [11,12]. Its

versatility has been demonstrated in the adsorption of various pollutants, including heavy metals and organic contaminants, from aqueous solutions [13]. However, the efficiency of BC as an adsorbent is highly dependent on the feedstock material and pyrolysis parameters [14]. Agricultural residues have emerged as a low-cost, environmentally friendly feedstock for BC production, yet the use of such biochars for CVOC removal has not been extensively investigated [15,16].

Date palm seed biochar (DPS-BC), derived from the pyrolysis of an abundant and underutilized byproduct in arid regions such as North Africa and the Middle East, presents unique advantages [17,18]. These include low production costs and high carbon yield, making it a promising alternative to traditional feedstocks. While substantial research has been conducted on biochars produced from wood and other agricultural residues, the specific application of DPS-BC for pollutant removal remains insufficiently explored. Notably, this research addresses a critical gap in the literature regarding DPS-BC's capacity to adsorb CVOCs, responding to the growing need for sustainable remediation technologies in regions rich in date palm waste [19].

Previous investigations have demonstrated the environmental applications of DPS-BC in various contexts. For example, Remmani et al. (2021) [15] successfully employed biochar derived from date palm residues for the removal of organic pollutants from oily wastewater, highlighting its strong adsorption capabilities for complex organics. Similarly, Mesnoua et al. (2021) [16] characterized biochars from date palm residues for soil amendment purposes, although their work did not explore water treatment applications. Building on these foundational studies, the doctoral research of one of this paper's authors [20] systematically examined the use of DPS-BC as an adsorbent for VOCs, specifically TCE and PCE. The present study takes this further by conducting a comparative analysis of DPS-BC and commercial activated carbon, optimizing pyrolysis conditions to enhance nanotube morphology and maximize adsorption performance. These advancements position DPS-BC as a high-performance, sustainable alternative to conventional adsorbents for CVOC remediation.

Recent advancements in pyrolysis techniques have demonstrated that optimizing biochar production to create nanotubular structures can significantly enhance adsorption performance by increasing surface area and improving pore accessibility [20]. These nanotube-structured biochars exhibit superior adsorption capacities for organic contaminants due to their unique geometrical features, which facilitate stronger interactions between the adsorbent and adsorbate [21,22]. However, the potential of nanotube-structured biochar derived from date palm seeds for CVOC remediation has been largely unexplored.

To address these gaps in the literature, we present an in-depth analysis of biochar synthesized from date palm seeds under optimized conditions to achieve nanotube morphology. This study systematically compares the adsorption efficiency of this novel biochar with that of commercial AC for the removal of TCE and PCE from aqueous solutions. Advanced kinetic and isotherm models were employed to elucidate underlying adsorption mechanisms, complemented by statistical analyses, including two-way ANOVA, to quantify the factors influencing adsorption performance [23]. By integrating innovative biochar synthesis techniques with comprehensive modeling and robust statistical validation, this research offers a thorough evaluation of biochar's potential as a sustainable and high-performance alternative to activated carbon for CVOC remediation, addressing a critical gap in the current body of knowledge.

2. Materials and Methods

2.1. Materials and Biochar Preparation

DPS of the Deglet Nour variety, an abundant agricultural byproduct in Algeria's Ziban region, was used as a raw material [10,24]. The Deglet Nour variety contributes significantly to the global date market, with Algeria producing millions of tons annually, and approximately 10–15% of this weight is seeds, which are often discarded as waste [10,24]. Leveraging this high-volume byproduct aligns with sustainability and circular economy

principles. The seeds were washed thoroughly, sun-dried, and ground into fine particles (<200 µm) to ensure uniformity for thermal treatment. The powdered seeds underwent pyrolysis in a fixed-bed reactor under limited oxygen conditions, reaching 828 °C at a heating rate of 10 °C per minute, maintained for 1.7 h. This temperature and duration were selected based on prior optimization studies using response surface methodology (RSM) to maximize surface area, porosity, and yield, crucial for environmental applications (Figure 1) [10,20]. Following pyrolysis, BC was washed with deionized water to remove impurities and oven-dried at 110 °C for 12 h, resulting in a carbon-rich material with high adsorption potential for contaminants [8,10,20].

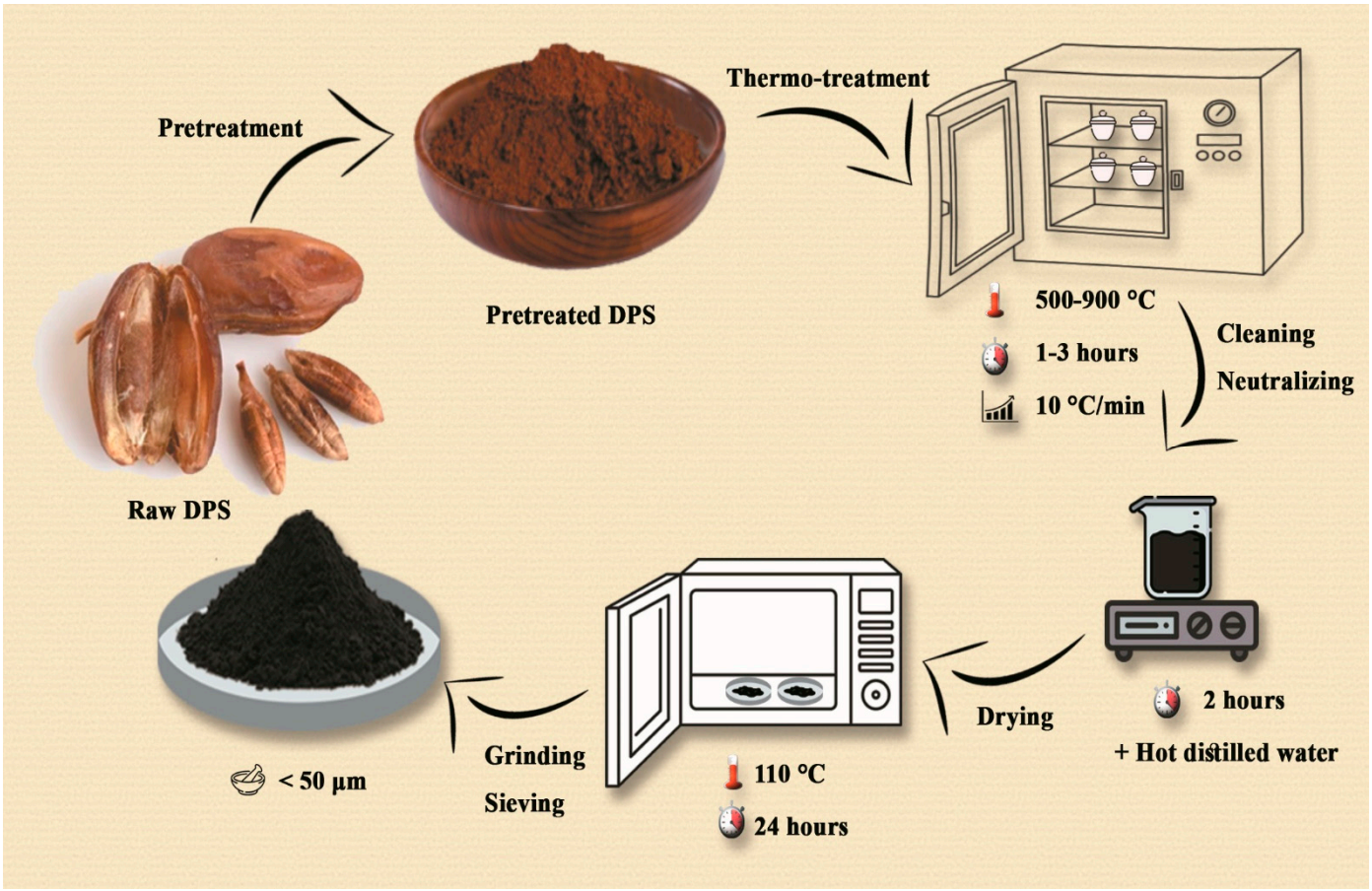

Figure 1. Synthesis journey and methodological innovation in BC preparation.

Additionally, the commercial activated carbon DARCO® Norit AC (Sigma-Aldrich®, −100 mesh, powder) was used as a benchmark in this comparative study. This AC has a high BET surface area, significant micropore volume, and moderate average pore size [25]. These properties make it an effective adsorbent in various environmental and industrial applications. Its physical and chemical characteristics have been previously detailed in studies where it has been employed as a support material for catalysts in hydrogenation reactions, showcasing its utility in enhancing surface reactions and adsorption processes. This AC was selected due to its widespread usage, standardized properties, and relevance to adsorption studies [25,26].

2.2. BC Characterization

To characterize the DPS-BC, scanning electron microscopy (SEM) was used to examine the surface morphology and confirm nanotube structures. The SEM analysis was conducted using a high-resolution microscope (SEM JSM-7610F Plus, JEOL, Zhubei, Taiwan), with magnifications ranging from ×1000 to ×2500 [11]. The Brunauer–Emmett–Teller (BET)

method was employed to determine the surface area and pore characteristics. Nitrogen adsorption–desorption isotherms were acquired at 77 K using a surface area analyzer (Micromeritics 3Flex Version 4.05, Micromeritics, Norcoss, GA, USA). The specific surface area was calculated using the BET equation, and the pore size distribution was derived using the Barrett–Joyner–Halenda (BJH) method, following Thommes et al. [10].

2.3. Batch Adsorption Tests

To ensure precision in the adsorption experiments for VOCs, a mono-component solution was prepared using Tedlar® bags while meticulously avoiding any headspace formation. High-purity VOCs (≥99.5% ACS grade, Sigma-Aldrich®, Steinheim, Germany) were measured with accuracy and introduced directly into the Tedlar® bags. This method ensured the attainment of the target concentration necessary for subsequent adsorption studies, providing a controlled and consistent environment for the experiments [20].

The batch adsorption tests conducted in this study encompassed a comprehensive evaluation of BC's adsorptive properties for CVOCs in aqueous solutions. The experimental design incorporated both kinetic and isotherm studies, utilizing carefully prepared mono-component CVOC solutions in Tedlar bags to maintain concentration integrity. The kinetic experiments were performed with an initial CVOC concentration of 50 mg/L and a solid/liquid ratio of 0.5, with triplicate sampling at intervals ranging from 0.5 to 28 h. The isotherm studies employed a range of initial CVOC concentrations (10–500 mg/L) and BC dosages (0.001–0.010 g), with a 24 h equilibration period determined from the kinetic results [27].

2.4. Determination of CVOCs

The concentrations of TCE and PCE were determined using a gas chromatography (GC) system, specifically the DANI MASTER instrument, Ramsey, MN, USA, which was equipped with a DANI 86.50 headspace auto-sampler for a precise and efficient sample introduction. The analytical setup featured a capillary column (TRB624, 30 m × 0.53 mm ID × 3 µm film thickness), optimized for VOC separation. Helium served as the carrier gas at a flow rate of 1.5 mL/min to ensure a robust performance and reliable peak resolution [20,28].

The temperature program for the GC oven was as follows: the initial temperature was 40 °C, maintained for 2 min, and this was followed by it being ramped up to 150 °C at a rate of 10 °C/min, where it was held for an additional 5 min. Injector and detector temperatures were set at 250 °C and 300 °C, respectively, to optimize analyte detection. Quantification was performed using a flame ionization detector (FID), providing high sensitivity for VOCs. Calibration curves were constructed using analytical-grade standards of TCE and PCE (purity ≥ 99.5%, Sigma-Aldrich®), ensuring accurate concentration measurements. Method detection limits (MDLs) for both the TCE and PCE were established according to the US EPA guidelines [20,29,30].

2.5. Modeling of Adsorption Process

The adsorption kinetics were modeled using both the pseudo-first-order (PFO) and pseudo-second-order (PSO) models, as described by Ho and McKay [23]. The PFO model is expressed as follows:

$$\log(q_e - q_t) = \log(q_e) - (k/2.303)t \quad (1)$$

where q_e and q_t are the adsorption capacities at equilibrium and the time t, respectively, and k is the rate constant. The PSO model, which accounts for chemisorption, is expressed as follows:

$$t/q_t = 1/(k.q_e^2) + (1/q_e)t \quad (2)$$

where k (g/mg·min) is the PSO rate constant. SigmaPlot 15.0 software was used for model fitting.

For equilibrium studies, the Langmuir and Freundlich isotherm models were applied [5]. The Langmuir model is expressed as follows:

$$q_e = (q_m K_L C_e)/(1 + K_L C_e) \quad (3)$$

where q_m (mg/g) is the maximum adsorption capacity and K_L (L/mg) is the Langmuir constant. The Freundlich model, which describes adsorption on heterogeneous surfaces, is given by the following:

$$qe = K_F C_e^{1/n} \quad (4)$$

where K_F and n are the Freundlich constants. SigmaPlot 15.0 software was used to fit the experimental data, and model selection was based on the coefficient of determination (R^2) and normalized root mean square error (NRMSE) [23].

2.6. Experimental Design and Statistical Analysis

A two-way analysis of variance (ANOVA) was performed using Design–Expert version 13 software to evaluate the effects of the adsorbent type (BC vs. AC) and contaminant type (TCE vs. PCE) on the adsorption capacity (Table 1). Statistical significance was set at $p < 0.05$. The ANOVA results were used to validate the significant superiority of BC in CVOC removal [10,11].

Table 1. Fitted models' data for kinetic study of CVOC adsorption into BC and AC.

Adsorbent Type	Contaminant Type	Q (mg/g)
AC	TCE	47.0061
BC	TCE	84.902
BC	PCE	83.2903
BC	PCE	83.4582
BC	TCE	84.953
AC	PCE	44.9667
BC	PCE	83.3743
AC	TCE	46.9642
AC	PCE	44.8889
AC	PCE	45.0128
BC	TCE	84.9296
AC	TCE	46.9293

3. Results and Discussion

3.1. BC and AC Characterization

Nitrogen adsorption–desorption isotherms and BET surface area analysis offer comprehensive insights into the porous structures and surface properties of BC and Norit Darco Sigma-Aldrich® AC. These two adsorbents exhibit distinct textural and morphological characteristics, which are critical for understanding their adsorption efficiencies in environmental applications. BC exhibits a Type IV isotherm with an H3 hysteresis loop, characteristic of materials combining mesopores and slit-shaped pores, as demonstrated in Figure 2 and Table 2. The BET surface area of the BC was measured at 654.79 m^2/g, which is significantly higher than most biochars typically reported in the literature, highlighting its enhanced adsorption capacity and reactivity. Its total pore volume was calculated at 0.1017 cm^3/g, with an average pore diameter of 3.09 nm, placing it within the mesoporous range (2–50 nm). These properties suggest a hierarchical pore structure where micropores (<2 nm) and mesopores coexist, which is advantageous for optimizing adsorption capacity and promoting efficient mass transfer kinetics [31]. At low relative pressures ($P/P^0 < 0.1$),

the sharp increase in adsorption reveals strong interactions with micropores, while the gradual uptake at moderate pressures indicates multilayer adsorption and capillary condensation within mesopores. The lack of a plateau at high relative pressures, coupled with the H3 hysteresis loop, underscores the presence of slit-like pores or aggregates of plate-like particles, enhancing the material's capability to adsorb larger molecules [32].

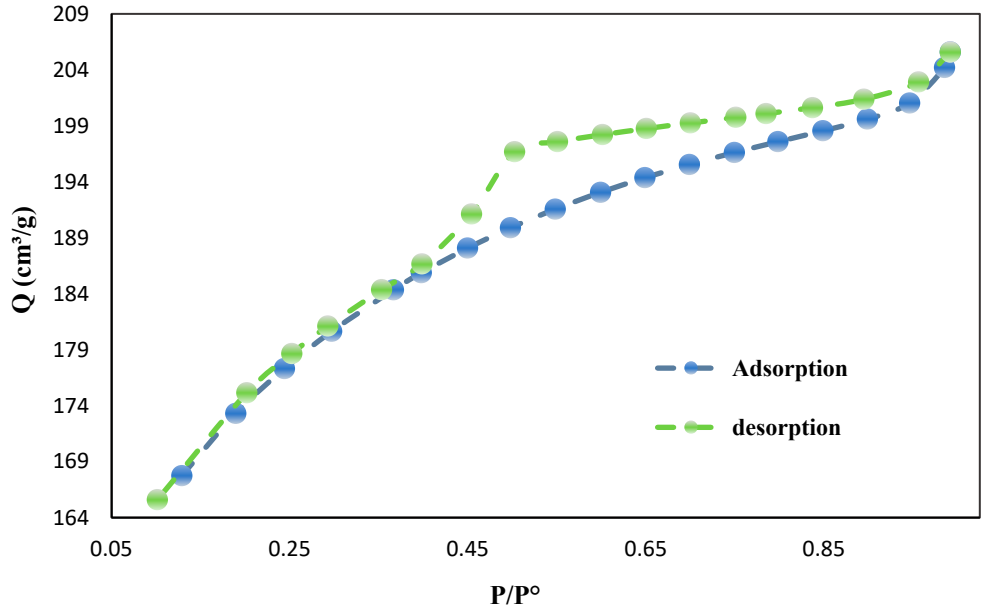

Figure 2. Nitrogen adsorption–desorption isotherm of BC.

Table 2. Physisorption characteristics and surface properties of BC and AC.

Parameter	Value	
Adsorbent	**BC**	**AC [25]**
BET (m^2/g)	654.79	876.45
Pore Volume (cm^3/g)	0.101	0.730
Pore Diameter (nm)	3.09	3.33

In comparison, the commercial AC displays similar mesoporous characteristics, as inferred from its Type IV isotherm and hysteresis. The BET surface area of the AC, derived from the literature [25], is reported as 876.45 m^2/g, significantly surpassing that of the BC. Its total pore volume of 0.73 cm^3/g and average pore diameter of 3.33 nm reflect its higher adsorption potential for both gas- and liquid-phase pollutants. This elevated surface area and larger pore volume suggest that the AC is particularly effective for rapid adsorption in high-capacity scenarios. However, the predominant mesoporosity of the AC, with a lower proportion of micropores, may limit its selectivity for smaller molecules compared to the BC [25]. Despite these differences, both the BC and AC demonstrate complementary adsorption properties. The BC's hierarchical pore structure and higher micropore content provide an edge in selective adsorption, particularly for small, polar molecules, while the AC's extensive surface area and higher mesopore fraction enhance its performance in applications requiring high-capacity, rapid adsorption. Such textural distinctions are critical in designing adsorbents tailored for specific environmental challenges, such as the removal of CVOCs or the sequestration of greenhouse gasses [30].

SEM analysis of the BC derived from date palm seed waste provided significant insights into its structural and morphological characteristics, illustrating a complex, hierarchical porous architecture. Its fibrillar surface morphology, as shown in Figure 3a,

highlights elongated, parallel strands, indicative of the partial preservation of the lignocellulosic structures of the precursor material after pyrolysis. This fibrillar morphology is critical as it contributes to the mechanical stability of the BC, enabling the retention of its porous network, which facilitates mass transfer and diffusion processes. Additionally, Figure 3b reveals a honeycomb-like porous network, showcasing the preservation of biological cell wall structures under controlled pyrolysis conditions. Such morphological features suggest that the thermal treatment parameters were well-optimized, preventing the collapse of the biomass's cellular architecture and ensuring the development of an interconnected pore network crucial for a large surface area and high adsorption efficiency.

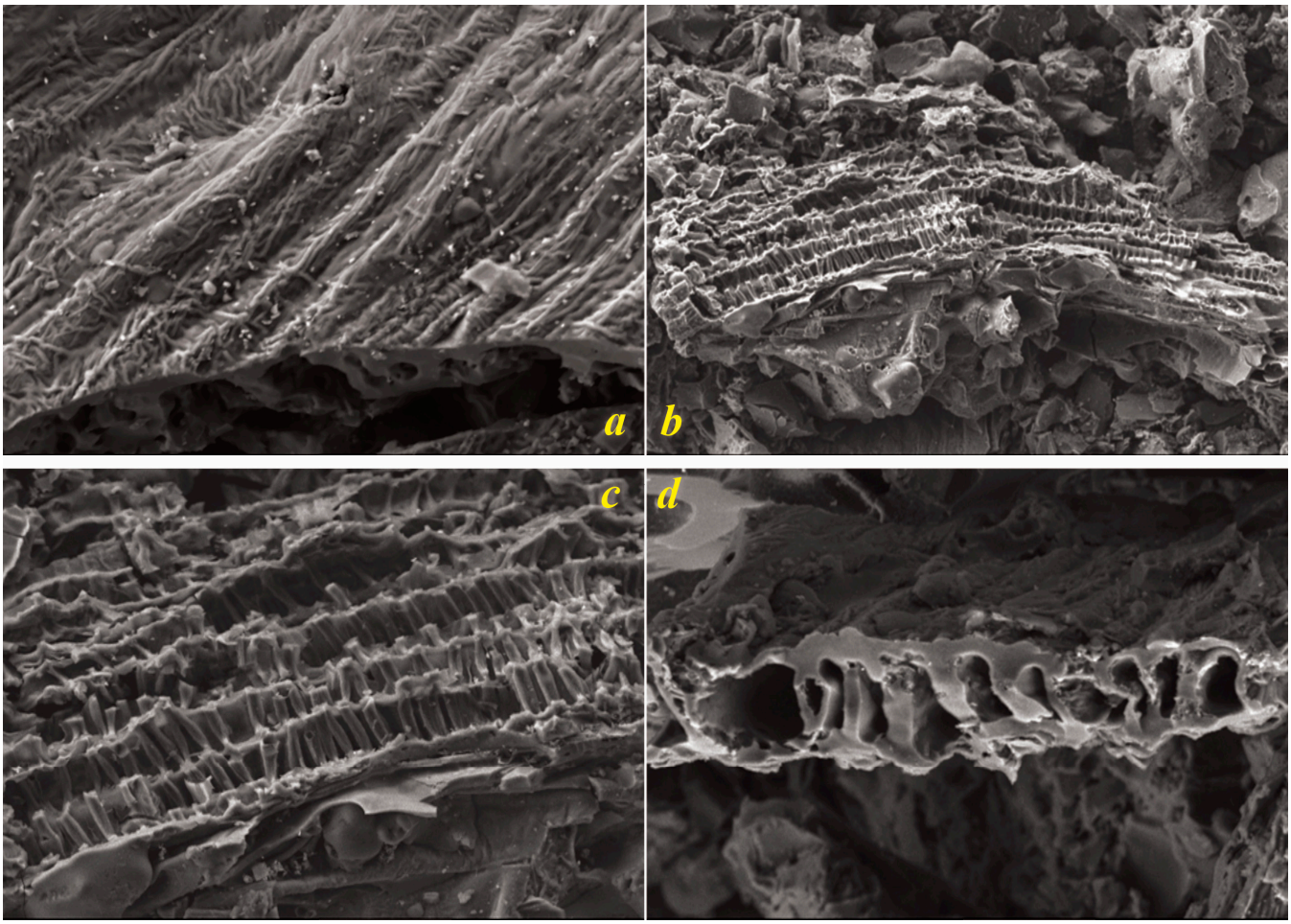

Figure 3. SEM micrograph of BC sample: (**a**) fibrillar surface morphology (magnification: ×2500; scale bar: 10 µm); (**b**) honeycomb-like porous network (magnification: ×1000; scale bar: 10 µm); (**c**) cross-sectional view of aligned porous structures (magnification: ×2500; scale bar: 10 µm); (**d**) high-magnification image of interconnected pores (magnification: ×2500; scale bar: 10 µm).

Further examination of the cross-sectional view (Figure 3c) and high-magnification details of the interconnected pores (Figure 3d) underscores the hierarchical nature of the porous system. The BC demonstrates a bimodal pore distribution, combining micropores and mesopores, which enhances its applicability in adsorption processes involving various pollutants. A high BET surface area of 654.79 m^2/g corroborates the effectiveness of the pyrolysis method in producing a material with substantial surface reactivity and adsorption capacity. These features are particularly advantageous for environmental remediation applications, as they allow for the adsorption of a broad range of contaminants, including CVOCs, which aligns with findings from recent studies on sustainable biochar development [33].

In comparison to chemical ACs, which often exhibit a more uniform microporous structure due to aggressive chemical treatments, the biochar described here maintains the inherent structural heterogeneity of the biomass. Previous studies, such as that by Singh et al. [25], have demonstrated that ACs typically undergo significant etching and pore development during activation processes, resulting in enhanced adsorption capabilities for small molecules but often at the expense of mechanical integrity. In contrast, the biochar's combination of mesoporosity and moderate microporosity provides a balanced system that can accommodate both small and large molecules, making it suitable for diverse applications, including water treatment, catalysis, and pollutant removal. Furthermore, the environmentally friendly preparation of BC, which avoids the use of harsh chemicals, presents a sustainable alternative to AC, addressing both environmental and economic concerns in material synthesis [30].

3.2. Kinetic Analysis of PCE and TCE Adsorption

The kinetic analysis of PCE and TCE adsorption into the synthesized BC and AC provided important insights into the mechanisms governing the adsorption process. Adsorption kinetics were modeled using both the PFO and PSO equations (Table 3). For PCE adsorption into the BC, the PSO model exhibited a better fit (R^2 = 0.9594) compared to the PFO model (R^2 = 0.7929), suggesting that chemisorption likely dominated the adsorption mechanism [6], where valence forces facilitated electron sharing or exchange between the adsorbate and adsorbent.

Table 3. Fitted models' data for kinetic study of CVOCs adsorption into BC and AC.

PCE Removal			
Fitted Model	Adsorbent	BC	AC
PFO	q (mg/g)	63.9401	44.7409
	K (min^{-1})	12.3923	6.8517
	R^2	0.7929	0.9998
PSO	q (mg/g)	85.9675	44.7409
	K (min^{-1})	0.0002	26,826.0932
	R^2	0.9594	0.9998
TCE Removal			
Fitted Model	Adsorbent	BC	AC
PFO	q (mg/g)	67.1037	44.9505
	K (min^{-1})	12.2270	7.1318
	R^2	0.8130	0.9843
PSO	q (mg/g)	86.6836	47.5400
	K (min^{-1})	0.0003	0.0031
	R^2	0.9810	0.9998

The theoretical maximum adsorption capacity for the PCE into the BC, as predicted by the PSO model, was 85.97 mg/g, substantially higher than the PFO estimate of 63.94 mg/g. This notable difference in capacity underscores the effectiveness of the BC, which can be attributed to its high specific surface area (654.79 m^2/g) and microporous structure [22]. Interestingly, the PSO rate constant (0.0002 min^{-1}) was significantly lower than the PFO constant (12.39 min^{-1}), indicating a more complex adsorption process. The initial stage likely involved rapid surface adsorption, followed by slower intraparticle diffusion into micropores, which may have acted as the rate-limiting step.

In contrast, the AC demonstrated a near-perfect fit to both the PFO and PSO models (R^2 = 0.9998), with identical adsorption capacities for the PCE (44.74 mg/g). The excep-

tionally high PSO rate constant for the AC (26,826.09 min^{-1}) suggested an extremely rapid adsorption process, likely facilitated by the highly developed and accessible pore network in the AC, leading to near-instantaneous equilibrium.

For TCE adsorption, similar trends were observed, with the BC showing a superior performance. The PSO model provided a better fit for TCE adsorption into the BC (R^2 = 0.9810) than the PFO model (R^2 = 0.8130), reinforcing the conclusion that chemisorption was the dominant mechanism. The PSO-predicted adsorption capacity for the TCE into the BC was 86.68 mg/g, slightly higher than for the PCE. This marginal increase was likely due to the smaller molecular size of the TCE, allowing for deeper penetration into the BC's microporous structure [34]. The rate constants for the TCE adsorption into the BC (12.23 min^{-1} for PFO and 0.0003 min^{-1} for PSO) were similar to those for the PCE, suggesting comparable adsorption kinetics for both chlorinated compounds.

For the AC, the PSO model again provided an excellent fit (R^2 = 0.9998) for TCE adsorption, with a slightly higher maximum adsorption capacity (47.54 mg/g) compared to the PCE (44.74 mg/g). The PSO rate constant for the TCE adsorption into the AC (0.0031 min^{-1}) was significantly lower than that observed for the PCE, indicating a slower adsorption process, possibly due to differences in the molecular interactions between the TCE and AC's surface.

Overall, the BC demonstrated superior adsorption capacities for both the PCE (85.97 mg/g) and TCE (86.68 mg/g) compared to the AC, which achieved capacities of 44.74 mg/g for the PCE and 47.54 mg/g for the TCE. These findings are consistent with Sun et al. (2023), who linked adsorption capacity variations to pore structure heterogeneity [35]. The superior performance of the BC can be attributed to its high surface area, well-developed microporosity, and nanotube structure, which collectively enhance its adsorption efficiency. The lower rate constants for the BC, especially in the PSO model, indicate that while the adsorption process was slower compared to the AC, the overall capacity was significantly greater due to the material's unique physicochemical properties.

The kinetic analysis of the PCE's and TCE's adsorption into the BC and AC revealed a strong correlation between their adsorption performance and structural characteristics. The BC exhibited superior adsorption capacities for the PCE and TCE compared to the AC. This enhanced performance is attributed to the BC's high surface area, microporous structure, and hierarchical pore distribution, which facilitate effective pollutant trapping and the deeper penetration of smaller molecules like TCE. In contrast, the AC's uniform and accessible pore network supported rapid adsorption kinetics, as evidenced by its higher PSO rate constant for the PCE. However, its lower surface area and less complex porosity limited its overall adsorption capacity.

The BC's adsorption process was better described by the PSO model, indicating a chemisorption mechanism involving electron sharing or exchange, while the AC's adsorption followed both the PFO and PSO models, reflecting simpler physical interactions. The slower adsorption rates of the BC, governed by intraparticle diffusion into micropores, highlighted the critical role of its tailored structural features. Conversely, the AC's chemical activation enhanced pore accessibility but reduced its ability to trap pollutants deeply, limiting its capacity despite rapid equilibrium attainment. These findings underscore BC's potential as a sustainable and efficient adsorbent for CVOCs, particularly in applications requiring high adsorption efficiency [3]. Meanwhile, AC remains advantageous for scenarios demanding rapid pollutant removal. This synergy between kinetic behavior and material properties emphasizes the suitability of BC as an eco-friendly alternative to conventional AC for environmental remediation.

3.3. Isotherm Modeling and Analysis

The adsorption isotherm studies provided crucial insights into the mechanisms governing the adsorption of TCE and PCE into both the BC and AC. The experimental data were fitted to both the Langmuir and Freundlich isotherm models, which offer complementary perspectives on adsorption behavior [36]. The results indicated that both models

demonstrated excellent fits, with high coefficients of determination ($R^2 > 0.98$) for all adsorption scenarios, revealing the complex nature of the adsorption process (Table 4).

Table 4. Fitted models' data for isotherm study of CVOC adsorption into BC and AC.

PCE Removal			
Adsorbent		BC	AC
Langmuir	Qmax (mg/g)	283.2054	593.1827
	K (L/mg)	0.1496	0.0046
	R^2	0.9862	0.9957
Freundlich	K (L/mg)	43.5601	3.1559
	n	0.6167	0.9187
	R^2	0.9940	0.9954
TCE Removal			
Adsorbent		BC	AC
Langmuir	Qmax (mg/g)	586.1234	713.4764
	K (L/mg)	0.0777	0.00856
	R^2	0.9984	0.9991
Freundlich	K (L/mg)	72.3580	7.8316
	n	0.4866	0.8534
	R^2	0.9826	0.9990

For PCE adsorption (Figure 4), the Freundlich model provided a slightly better fit for both the BC ($R^2 = 0.9940$) and AC ($R^2 = 0.9954$) compared to the Langmuir model (BC: $R^2 = 0.9862$; AC: $R^2 = 0.9957$). This suggests that the PCE adsorption on both adsorbents was primarily governed by multilayer adsorption on heterogeneous surfaces [6]. The Freundlich constant (K) for the BC was substantially higher (43.56 L/mg) than for the AC (3.16 L/mg), indicating a much stronger affinity of the PCE for the BC, particularly at lower equilibrium concentrations. The Freundlich exponents (n) for both adsorbents were less than unity (BC: 0.6167; AC: 0.9187), indicating favorable adsorption conditions, although the lower n value for the BC implied a more heterogeneous surface with a broader distribution of adsorption site energies. This aligns with the observed complex nanotube structure of the BC, which contributes to its heterogeneous adsorption properties [36].

For TCE adsorption (Figure 5), both models also demonstrated excellent fits; however, the Langmuir model exhibited a marginally better fit for the BC ($R^2 = 0.9984$) than the Freundlich model ($R^2 = 0.9826$). This slight preference for the Langmuir model suggests that TCE adsorption into the BC may have involved more uniform monolayer adsorption on relatively homogeneous surface sites, likely due to specific interactions between the TCE molecules and the nanotube structures observed in the SEM analysis. For the AC, both models provided nearly identical fits (Freundlich $R^2 = 0.9990$; Langmuir $R^2 = 0.9991$), reflecting a more complex adsorption mechanism that likely included both monolayer and multilayer adsorption processes.

The maximum adsorption capacities (Qmax) predicted by the Langmuir model provided further insight into the adsorbents' performance. For the PCE, the BC exhibited a Qmax of 283.21 mg/g, which was approximately 48% of the AC's capacity (593.18 mg/g). However, for the TCE, the BC showed a significantly higher Qmax of 586.12 mg/g, reaching approximately 82% of the AC's capacity (713.48 mg/g). This remarkable performance of the BC in the TCE adsorption was notable, especially considering that the BC was derived from a waste material and required less extensive activation compared to the AC.

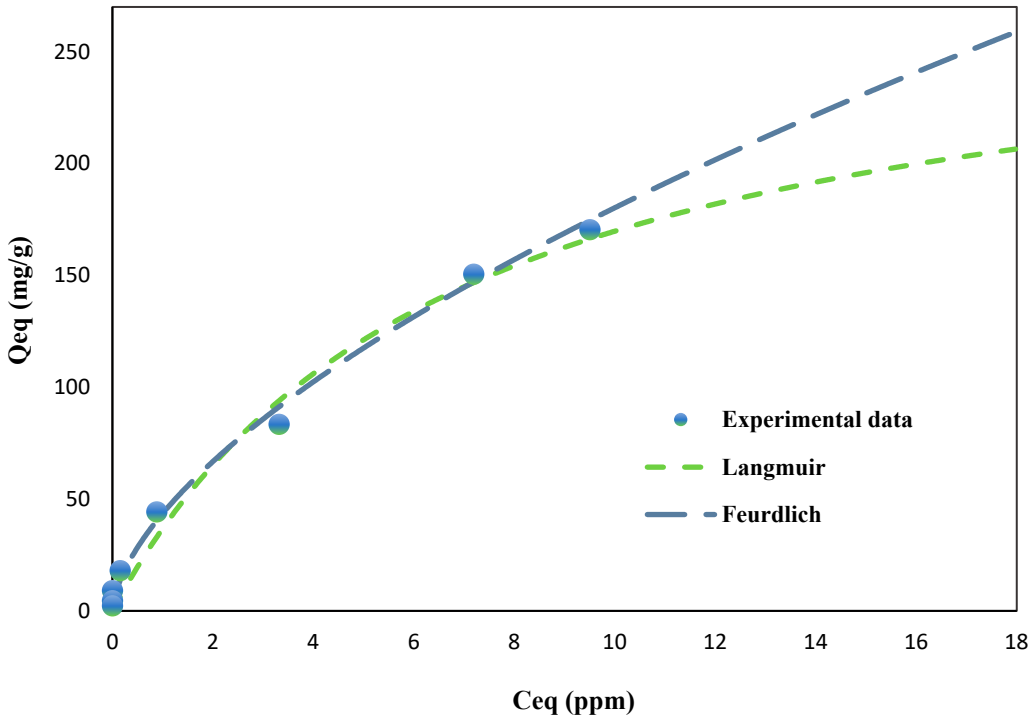

Figure 4. Isotherm presentation of PCE adsorption into BC: experimental data and Freundlich and Langmuir isotherms.

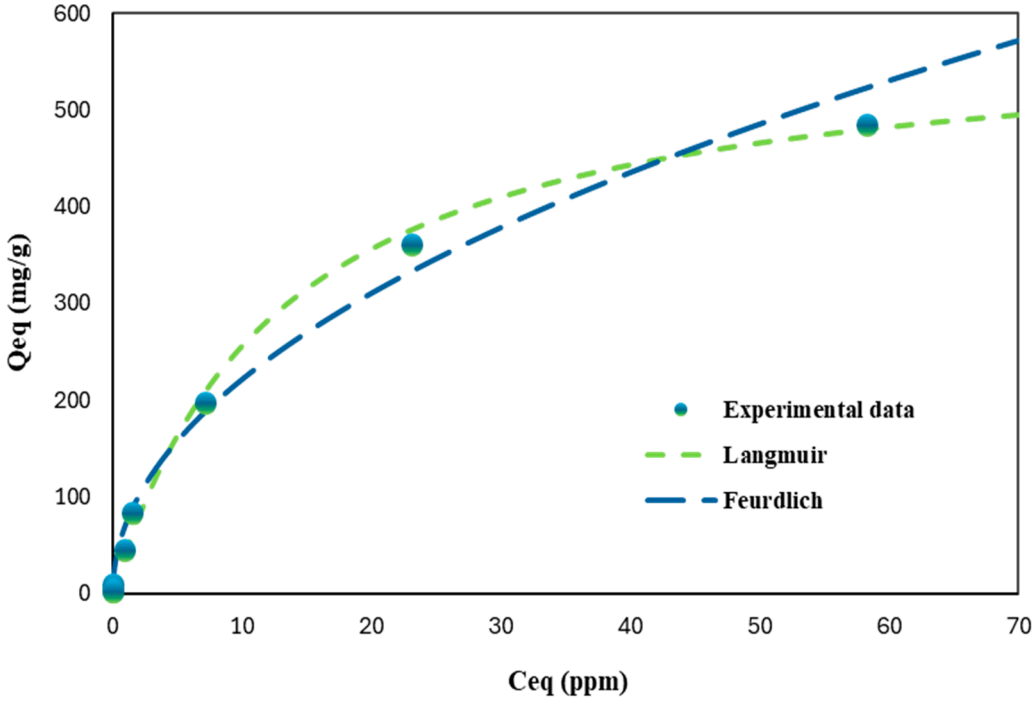

Figure 5. Isotherm presentation of TCE adsorption into BC: experimental data and Freundlich and Langmuir isotherms.

The higher adsorption capacity of the BC for the TCE compared to the PCE could be attributed to several factors, including the smaller molecular size of the TCE (molecular weight: 131.39 g/mol) compared to the PCE (molecular weight: 165.83 g/mol), which likely allowed for better penetration into the BC's micropores. Additionally, the unique nanotube morphology of the BC may have promoted stronger π-π interactions between the TCE and the graphitic domains within the biochar's amorphous carbon structure. These interactions

were likely more pronounced for the TCE due to its higher electron density, resulting in stronger adsorbate–adsorbent interactions [37].

The Langmuir constant (K), which reflects the affinity between an adsorbate and adsorbent, was higher for the BC than for the AC for both the PCE (BC: 0.1496 L/mg; AC: 0.0046 L/mg) and TCE (BC: 0.0777 L/mg; AC: 0.0086 L/mg), suggesting that the BC exhibited stronger binding energies with both chlorinated compounds. This enhanced affinity was likely due to the diverse surface functionalities present on the BC, as identified through FTIR analysis during the characterization phase of this study. The higher K value for the PCE with the BC compared to the TCE might be explained by the increased polarizability of the PCE, which could have enhanced its interaction with the polar functional groups on the BC's surface.

The observed differences in adsorption behavior between the TCE and PCE may also be related to their aqueous solubilities and hydrophobicities. TCE, with a higher solubility in water (1280 mg/L at 25 °C) compared to PCE (150 mg/L at 25 °C), tends to remain in the aqueous phase for longer periods. However, the high adsorption capacity of the BC for the TCE suggests that the adsorbent–adsorbate interactions overcame the solvent–adsorbate interactions effectively. Additionally, PCE's higher hydrophobicity (log Kow = 3.40) compared to TCE (log Kow = 2.42) could explain its stronger affinity for the hydrophobic regions of the BC, as indicated by the higher Freundlich K value for the PCE [37–39].

Overall, the isotherm analysis reveals that BC demonstrates strong potential as a sustainable and high-performance adsorbent for chlorinated VOCs [22]. The distinct adsorption behavior between the TCE and PCE highlights the importance of considering molecular properties in adsorption processes, while the high surface area and unique pore structure of BC enhance its efficacy in CVOC remediation [23,24,27].

3.4. Comparative Analysis of BC and AC for CVOC Adsorption: ANOVA Approach

The statistical analysis of the adsorption capacities for the BC and AC in removing the TCE and PCE was performed using an ANOVA approach. This analysis revealed significant main effects for both types of adsorbent and types of contaminant, as well as a notable interaction between these two factors, thereby providing a comprehensive evaluation of the factors affecting adsorption efficiency [40,41] (Figure 6).

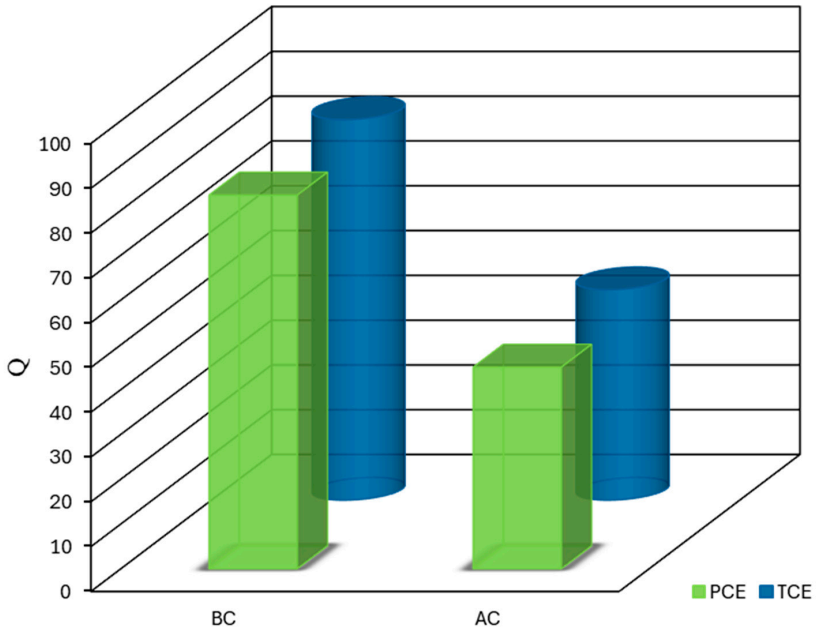

Figure 6. Comparative adsorption capacities of BC and AC for TCE and PCE.

The type of adsorbent emerged as the most critical factor influencing adsorption capacity, as indicated by an extremely high F-value ($F = 1.336 \times 10^6$; $p < 0.0001$). This finding underscores the substantial role that the choice between BC and AC plays in the efficiency of CVOC removal. The negative coefficient estimate for the adsorbent factor (−19.09) indicates that the BC consistently demonstrated superior adsorption capacity compared to the AC for both the TCE and PCE [42]. This was reflected in the mean adsorption capacities, with the BC showing remarkably higher capacities for both contaminants, thereby outperforming the AC in all cases.

Although less pronounced, the contaminant type also had a significant effect on the adsorption capacity ($F = 2909.53$; $p < 0.0001$). The positive coefficient estimate (0.89) for this factor indicates that, on average, the TCE was adsorbed to a slightly greater extent than the PCE across both adsorbents. While this difference was statistically significant, it is relatively minor in practical terms. This variation in adsorption performance can be attributed to the molecular properties of TCE and PCE, with TCE's smaller molecular size and higher polarity potentially enhancing its interactions with adsorbent surfaces [43], particularly in BC's microporous structure. This observation is consistent with prior studies on the selective adsorption of chlorinated organics [29].

In addition, a significant interaction between the adsorbent type and the contaminant type was observed ($F = 47.72$; $p = 0.0001$). The positive coefficient estimate for this interaction term (0.11) suggests that the effect of the adsorbent type on adsorption capacity was slightly moderated by the type of contaminant and vice versa [5]. Although statistically significant, this interaction had a considerably smaller magnitude than the main effects. The presence of this interaction suggests that the relative performance of the BC and AC may have varied depending on the specific contaminant, although the BC exhibited more consistent performance across both the TCE and PCE.

The ANOVA model demonstrated excellent predictive capabilities, as indicated by its R-squared and adjusted R-squared values of 1.0000, which confirmed the robustness of the model [44]. The predicted R-squared was in perfect agreement with the adjusted R-squared, highlighting the model's reliability. Additionally, the high adequate precision ratio (1209.817) far exceeded the desirable threshold of 4, indicating a strong signal-to-noise ratio, further validating the accuracy of the model within the design space. The low standard error of the coefficient estimates (0.017) for all factors and their interaction confirmed the precision of the model's predictions.

These statistical findings have substantial implications for the remediation of chlorinated VOCs. The marked superiority of the BC over the AC in the adsorption of both the TCE and PCE strongly supports the use of biochar derived from date palm seeds as a preferred adsorbent for CVOC removal from aqueous solutions. The magnitude of this effect suggests that switching from AC to BC could significantly enhance remediation efficacy. While both adsorbents showed a slight preference for the TCE over the PCE, this difference was more pronounced for the AC, suggesting that BC offers more consistent performance across a variety of CVOCs. This consistent behavior of BC could be particularly advantageous in treating mixed-contaminant environments, which are common in real-world applications [16,27].

The small but significant interaction effect between the adsorbent type and contaminant type suggests that optimizing adsorption processes may require the consideration of the specific contaminants present. However, the dominant influence of the adsorbent type indicates that BC is likely to outperform AC in a wide range of scenarios. Given BC's superior performance, its use as a sustainable alternative to AC has substantial environmental benefits [45]. Producing BC from agricultural waste, such as date palm seeds, not only enhances the environmental sustainability of water treatment technologies but also promotes the valorization of waste materials, potentially reducing the carbon footprint of adsorbent production [10,20].

4. Conclusions

This research marks a significant advancement in the field of environmental remediation, specifically for the removal of CVOCs from aqueous solutions. The study underscores the potential of date-palm-seed-derived BC as a sustainable and highly efficient alternative to conventional AC, offering a dual benefit of environmental protection and waste valorization.

The optimized BC exhibited exceptional adsorption capacities, achieving 86.68 mg/g for the TCE and 85.97 mg/g for the PCE, significantly outperforming the commercial AC across all experimental conditions. Its remarkable performance was attributed to its unique structural properties, including a high BET surface area of 654.79 m^2/g, well-developed microporosity, and distinctive nanotube morphology, as confirmed by detailed the SEM and BET analyses. These features provided a robust framework for effective adsorption through enhanced surface interactions and supported both multilayer and monolayer adsorption processes.

The adsorption mechanisms were elucidated through kinetic and isotherm modeling, where the pseudo-second-order kinetic model highlighted chemisorption as the dominant mechanism. The Freundlich and Langmuir isotherm models demonstrated strong fits, indicating a combination of heterogeneous surface adsorption and multilayer formation. Additionally, statistical validation using two-way ANOVA confirmed the significant superiority of the BC over the AC ($p < 0.0001$), with further insights into interactions between the adsorbent type and contaminant type reinforcing the reliability of the results.

Beyond laboratory-scale success, this study emphasizes the broader implications of using agricultural waste to produce high-performance adsorbents. By transforming readily available date palm seeds into advanced biochar materials, this approach offers a cost-effective and environmentally sustainable solution for water treatment technologies. These findings provide a robust foundation for future innovations in the development of sustainable adsorbents, with promising applications in large-scale water purification and pollution mitigation systems.

Author Contributions: Conceptualization, R.R.; Funding acquisition, M.P.P. and A.R.C.; Investigation, R.R.; Resources, M.P.P.; Software, R.R. and N.A.; Supervision, M.P.P. and N.A.; Validation, R.R.; Visualization, R.R. and M.P.P.; Writing—original draft, R.R. and N.A.; Writing—review and editing, R.R. and A.R.C. All authors have read and agreed to the published version of the manuscript.

Funding: This research received no external funding.

Data Availability Statement: The original contributions presented in this study are included in the article. Further inquiries can be directed to the corresponding author.

Acknowledgments: The authors extend their sincere gratitude to the Scientific and Technical Research Center for Arid Regions (CRSTRA) in Biskra, Algeria, for facilitating the biochar preparation and initial experimental work. We also express our appreciation to the Laboratory of Sustainable Processes (Chemical and Biological) for Environmental Recovery and Protection at Sapienza University of Rome, Italy, where the adsorption tests were conducted.

Conflicts of Interest: The authors declare no conflicts of interest.

References

1. Jatoi, A.S.; Ahmed, J.; Bhutto, A.A.; Jeyapaul, A.S. Recent advances and future perspectives of carbon-based nanomaterials for environmental remediation. *Braz. J. Chem. Eng.* **2024**, 1–19. [CrossRef]
2. Pandey, P.; Yadav, R. A review on volatile organic compounds (VOCs) as environmental pollutants: Fate and distribution. *Int. J. Plant Environ.* **2018**, *4*, 14–26. [CrossRef]
3. Song, Q.; Kong, F.; Liu, B.F.; Song, X.; Ren, H.Y. Biochar-based composites for removing chlorinated organic pollutants: Applications, mechanisms, and perspectives. *Environ. Sci. Ecotechnol.* **2024**, *21*, 100420. [CrossRef]
4. Hussain, B.; Chen, J.-S.; Huang, S.-W.; Tsai, I.-S.; Rathod, J.; Hsu, B.-M. Underpinning the ecological response of mixed chlorinated volatile organic compounds (CVOCs) associated with contaminated and bioremediated groundwaters: A potential nexus of microbial community structure and function for strategizing efficient bioremediation. *Environ. Pollut.* **2023**, *334*, 122215. [CrossRef] [PubMed]

5. Foo, K.Y.; Hameed, B.H. Insights into the modeling of adsorption isotherm systems. *Chem. Eng. J.* **2010**, *156*, 2–10. [CrossRef]
6. Rashid, R.; Shafiq, I.; Akhter, P.; Iqbal, M.J.; Hussain, M. A state-of-the-art review on wastewater treatment techniques: The effectiveness of the adsorption method. *Environ. Sci. Pollut. Res.* **2021**, *28*, 9050–9066. [CrossRef]
7. Brusseau, M.L.; Carroll, K.C.; Truex, M.J.; Becker, D.J. Characterization and remediation of chlorinated volatile organic contaminants in the vadose zone. *Vadose Zone J.* **2013**, *12*, vzj2012.0137. [CrossRef]
8. Qiu, B.; Shao, Q.; Shi, J.; Yang, C.; Chu, H. Application of biochar for the adsorption of organic pollutants from wastewater: Modification strategies, mechanisms, and challenges. *Sep. Purif. Technol.* **2022**, *300*, 121925. [CrossRef]
9. Seow, Y.X.; Tan, Y.H.; Mubarak, N.M.; Kansedo, J.; Khalid, M.; Ibrahim, M.L.; Ghasemi, M. A review on biochar production from different biomass wastes by recent carbonization technologies and its sustainable applications. *J. Environ. Chem. Eng.* **2022**, *10*, 107017. [CrossRef]
10. Remmani, R.; Yilmaz, M.; Benaoune, S.; Di Palma, L. Optimized pyrolytic synthesis and physicochemical characterization of date palm seed biochar: Unveiling a sustainable adsorbent for environmental remediation applications. *Environ. Sci. Pollut. Res.* **2024**, *31*, 60065–60079. [CrossRef] [PubMed]
11. Díaz, B.; Sommer-Márquez, A.; Ordoñez, P.E.; Bastardo-González, E.; Ricaurte, M.; Navas-Cárdenas, C. Synthesis methods, properties, and modifications of biochar-based materials for wastewater treatment: A review. *Resources* **2024**, *13*, 8. [CrossRef]
12. Thommes, M.; Kaneko, K.; Neimark, A.V.; Olivier, J.P.; Rodriguez-Reinoso, F.; Rouquerol, J.; Sing, K.S.W. Physisorption of gases with special reference to the evaluation of surface area and pore size distribution (IUPAC Technical Report). *Pure Appl. Chem.* **2015**, *87*, 1051–1069. [CrossRef]
13. Al Masud, M.A.; Shin, W.S.; Sarker, A.; Septian, A.; Das, K.; Deepo, D.M.; Malafaia, G. A critical review of sustainable application of biochar for green remediation: Research uncertainty and future directions. *Sci. Total Environ.* **2023**, *904*, 166813. [CrossRef]
14. Mistry, N.; Patel, V.; Parekh, P.; Naik, P.; Kumar, N.S.; Vekariya, R.; Khimani, M. Adsorbent materials. In *Materials from Natural Sources*; CRC Press: Boca Raton, FL, USA, 2024; pp. 20–45.
15. Remmani, R.; Makhloufi, R.; Miladi, M.; Ouakouak, A.; Canales, A.R.; Núñez-Gómez, D. Development of low-cost activated carbon towards an eco-efficient removal of organic pollutants from oily wastewater. *Pol. J. Environ. Stud.* **2021**, *30*, 1801–1808. [CrossRef]
16. Mesnoua, M.; Remmani, R.; Benchik, C. Characterization of slow pyrolysis biochars from date palm residues with the aim of soil amendment. *J. Environ. Manag.* **2021**, *247*, 1–8.
17. Al-Karmadi, A.; Okoh, A.I. An overview of date (Phoenix dactylifera) fruits as an important global food resource. *Foods* **2024**, *13*, 1024. [CrossRef]
18. Abid, W.; Ammar, E. Date palm (*Phoenix dactylifera* L.) wastes valorization: A circular economy approach. In *Mediterranean Fruits Bio-Wastes: Chemistry, Functionality and Technological Applications*; Springer: Cham, Switzerland, 2022; pp. 403–430.
19. Zhou, Y.; Qin, S.; Verma, S.; Sar, T.; Sarsaiya, S.; Ravindran, B.; Awasthi, M.K. Production and beneficial impact of biochar for environmental application: A comprehensive review. *Bioresour. Technol.* **2021**, *337*, 125451. [CrossRef]
20. Remmani, R. Optimization and Application of Date Palm Seed Derived Biochar for Augmented Adsorption of Volatile Organic Compounds: A Specialized Inquiry into Trichloroethylene (TCE) and Tetrachloroethylene (PCE) Remediation. Doctoral Dissertation, Université Mohamed Khider, Biskra, Algérie, 2024. [CrossRef]
21. Nunes, C.A.; Guerreiro, M.C. Estimation of surface area and pore volume of activated carbons by methylene blue and iodine numbers. *Quim. Nova* **2011**, *34*, 472–476. [CrossRef]
22. Amalina, F.; Krishnan, S.; Zularisam, A.W.; Nasrullah, M. Recent advancement and applications of biochar technology as a multifunctional component towards sustainable environment. *Environ. Dev.* **2023**, *46*, 100819. [CrossRef]
23. Ho, Y.S.; McKay, G. Pseudo-second order model for sorption processes. *Process Biochem.* **1999**, *34*, 451–465. [CrossRef]
24. Roumani, M.; Remmani, R.; Miladi, M.; Abu-Khalaf, N.; Canales, A.R. Physical properties and mass models of Deglet Noor and Arichti semi-dry Algerian date fruits: A comparative study. *Food Sci. Nutr.* **2024**, *12*, 2886–2895. [CrossRef] [PubMed]
25. Singh, G.; Pant, K.K. Catalytic CO2 adsorption and hydrogenation using activated carbon supported catalysts. *Appl. Catal. B Environ.* **2017**, *203*, 358–370. [CrossRef]
26. Capelli, S.; Motta, D.; Evangelisti, C.; Dimitratos, N.; Prati, L.; Pirola, C.; Villa, A. Effect of carbon support, capping agent amount, and Pd NPs size for bio-adipic acid production from muconic acid and sodium muconate. *Nanomaterials* **2020**, *10*, 505. [CrossRef]
27. Rossi, M.M.; Silvani, L.; Amanat, N.; Petrangeli Papini, M. Biochar from pine wood, rice husks, and iron-eupatorium shrubs for remediation applications: Surface characterization and experimental tests for trichloroethylene removal. *Materials* **2021**, *14*, 1776. [CrossRef] [PubMed]
28. Epping, R.; Koch, M. On-site detection of volatile organic compounds (VOCs). *Molecules* **2023**, *28*, 1598. [CrossRef] [PubMed]
29. U.S. Environmental Protection Agency. *Definition and Procedure for the Determination of the Method Detection Limit*; Revision 2; (EPA 821-R-16-006); U.S. Environ. Prot. Agency: Washington, DC, USA, 2016.
30. Grocki, P.; Davis, M.D.; Agarwal, M. Methods to detect volatile organic compounds for breath biopsy using solid-phase micro-extraction and gas chromatography–mass spectrometry. *Molecules* **2023**, *28*, 4533. [CrossRef]
31. Yin, Y.; Liu, Q.; Zhao, Y.; Chen, T.; Wang, J.; Gui, L.; Lu, C. Recent progress and future directions of biomass-derived hierarchical porous carbon: Designing, preparation, and supercapacitor applications. *Energy Fuels* **2023**, *37*, 3523–3554. [CrossRef]
32. Al-Ghouti, M.A.; Khan, M.; Alhattab, M. Sustainable activated carbon synthesis and its adsorptive properties for environmental pollutants. *Sustainability* **2022**, *14*, 6712. [CrossRef]

33. Sahoo, P.K.; Datta, R.; Rahman, M.M.; Sarkar, D. Sustainable environmental technologies: Recent development, opportunities, and key challenges. *Appl. Sci.* **2024**, *14*, 10956. [CrossRef]
34. Xiang, Y.; Lu, L.; Kottapalli, A.G.P.; Pei, Y. Status and perspectives of hierarchical porous carbon materials in terms of high-performance lithium–sulfur batteries. *Carbon Energy* **2022**, *4*, 346–398. [CrossRef]
35. Sharma, G.; Sharma, S.; Kumar, A.; Lai, C.W.; Naushad, M.; Shehnaz; Iqbal, J.; Stadler, F.J. Activated carbon as superadsorbent and sustainable material for diverse applications. *Adsorpt. Sci. Technol.* **2022**, *2022*, 4184809. [CrossRef]
36. Lai, K.C.; Zhang Hiew, B.Y.; Tee, W.T.; Thangalazhy-Gopakumar, S.; Gan, S.; Lee, L.Y. Usage of a new macro-hierarchical graphene sponge in batch adsorption and packed column configuration for efficient decontamination of cadmium in aqueous environment. *J. Environ. Chem. Eng.* **2021**, *9*, 106057. [CrossRef]
37. Han, L.; Qian, L.; Yan, J.; Chen, M. Effects of the biochar aromaticity and molecular structures of the chlorinated organic compounds on the adsorption characteristics. *Environ. Sci. Pollut. Res.* **2017**, *24*, 5554–5565. [CrossRef] [PubMed]
38. Sankaranarayanan, S.; Lakshmi, D.S.; Vivekanandhan, S.; Ngam-charussrivichai, C. Biocarbons as emerging and sustainable hydrophobic/oleophilic sorbent materials for oil/water separation. *Sustain. Mater. Technol.* **2021**, *28*, e00268. [CrossRef]
39. Jeirani, Z.; Niu, C.H.; Soltan, J. Adsorption of emerging pollutants on activated carbon. *Rev. Chem. Eng.* **2017**, *33*, 491–522. [CrossRef]
40. Das, A.; Mondal, S.; Hansda, K.M.; Adak, M.K.; Dhak, D. A critical review on the role of carbon supports of metal catalysts for selective catalytic hydrogenation of chloronitrobenzenes. *Appl. Catal. A Gen.* **2023**, *649*, 118955. [CrossRef]
41. Bhatti, A.H.; Waris, M.; Kazmi, W.W.; Bhatti, U.H.; Min, G.H.; Park, B.C.; Kweon, S.; Baek, I.H.; Nam, S.C. Metal impregnated activated carbon as cost-effective and scalable catalysts for amine-based CO_2 capture. *J. Environ. Chem. Eng.* **2023**, *11*, 109231. [CrossRef]
42. Yang, L.; Takkallapally, C.; Gabhi, R.S.; Jiang, W.; Kirk, D.W.; Jia, C.Q. Wood biochar monolith-based approach to increasing the volumetric energy density of supercapacitor. *Ind. Eng. Chem. Res.* **2022**, *61*, 7891–7901. [CrossRef]
43. Li, L.; Quinlivan, P.A.; Knappe, D.R.U. Effects of activated carbon surface chemistry and pore structure on the adsorption of organic contaminants from aqueous solution. *Carbon* **2002**, *40*, 2085–2100. [CrossRef]
44. Young, P.C.; Ratto, M. A unified approach to environmental systems modeling. *Stoch. Environ. Res. Risk Assess.* **2009**, *23*, 1037–1057. [CrossRef]
45. Khan, N.; Chowdhary, P.; Gnansounou, E.; Chaturvedi, P. Biochar and environmental sustainability: Emerging trends and techno-economic perspectives. *Bioresour. Technol.* **2021**, *332*, 125102. [CrossRef] [PubMed]

Disclaimer/Publisher's Note: The statements, opinions and data contained in all publications are solely those of the individual author(s) and contributor(s) and not of MDPI and/or the editor(s). MDPI and/or the editor(s) disclaim responsibility for any injury to people or property resulting from any ideas, methods, instructions or products referred to in the content.